

**DESIGN AND EVALUATION OF ARTIFICIAL
CATALYSTS THAT POSSESS ENZYME-LIKE
AMIDOLYTIC CATALYSIS**

WONG YOKE MING

UNIVERSITI SAINS MALAYSIA

2017

**DESIGN AND EVALUATION OF ARTIFICIAL
CATALYSTS THAT POSSESS ENZYME-LIKE
AMIDOLYTIC CATALYSIS**

by

WONG YOKE MING

**Thesis submitted in fulfillment of the requirements
for the degree of
Doctor of Philosophy**

November 2017

ACKNOWLEDGEMENT

First of all, I would like to express my deepest appreciation and sincere gratitude to my supervisor, Prof. Dr. K. Sudesh Kumar for his continuous support and resolute guidance throughout my PhD project. Thanks for the opportunity given to me for pursuing my study in RIKEN, Japan.

I would like to thank my co-supervisor, Dr. Keiji Numata. His valuable advice, information, patience, and constructive suggestion have guided me in completing my PhD project successfully. I am grateful to him for providing me this challenging project title to complete my PhD degree study in RIKEN, Japan.

I am deeply indebted to my colleagues in Enzyme Research Team, RIKEN, especially Dr. Jo-Ann Chuah, Dr. Peter James Baker, Dr. Jose Ageitos, Shoya Yamazaki, and Kumiko Morisaki for their unlimited guidance, advice, contribution and assistants to the achievement of my study. It is with particular pleasure that I thank the Research Officers of Ecobiomaterial Laboratory, Dr. Jiun Yee Chee, Dr Diana Ch'ng and Ms. Ferryn Ooi for helping me in handling all the candidature matters during my PhD attachment in RIKEN, Japan.

I wish to thank Universiti Sains Malaysia for the Fellowship and RIKEN for the scholarship and opportunity to carry out this work as International Program Associate.

Last but not least, I am extremely grateful to my lovely family for their encouragement, tolerance and boundless moral support that keep my spirits up and enable me to go through all the obstacles throughout my PhD project.

WONG YOKE MING

TABLE OF CONTENTS

ACKNOWLEDGEMENT	ii
TABLE OF CONTENTS	iii
LIST OF TABLES	vi
LIST OF FIGURES	vii
LIST OF ABBREVIATIONS	xiv
ABSTRAK	xvi
ABSTRACT	xviii
CHAPTER ONE:INTRODUCTION	1
1.1 General Introduction	1
1.2 Hypothesis and Aims of Thesis	3
CHAPTER TWO: LITERATURE REVIEW	4
2.1 Native Enzymes and Its Mechanisms	4
2.1.1 Proteases	4
2.1.1(a) Serine Proteases	7
2.1.1(b) Cysteine Proteases	9
2.1.1(c) Aspartic Proteases	11
2.1.1(d) Metalloproteases	12
2.1.1(e) Protease-mediated Polypeptides Synthesis	12
2.2 Artificial Catalyst	16
2.2.1 Artificial Catalysts Based on Random Copolymers	21
2.2.1(a) <i>N</i> -isopropylacrylamide (NIPAm)	22
2.2.2 Artificial Catalyst Based On Imprinted Polymers	25
2.2.3 Artificial Catalysts Based On Self-assembled Short Peptides	28

CHAPTER THREE: EVALUATION OF POLY(<i>N</i>-ISOPROPYLACRYLAMIDE) MICROGEL AS AN ARTIFICIAL AMIDASE	32
3.1 Introduction	32
3.2 Materials and Methods	33
3.2.1 Materials	33
3.2.2 NMG Synthesis	33
3.2.3 NMG Characterization	35
3.2.4 Amidolytic Activity Measurement	36
3.2.5 Inhibition Assay	38
3.3 Results and Discussion	39
3.3.1 NMG Characterization	39
3.3.2 Evaluation of NMG Concentration	42
3.3.3 Protonation and Deprotonation of the Functional Groups	45
3.3.4 Density of the Functional Groups	51
3.3.5 Substrate Specificity Study	53
3.3.6 Proposed Mechanism of Amidolytic Activity and Theoretical Average Distance Between Functional Groups in NMG	58
3.3.7 Inhibition Assay	65
CHAPTER FOUR: ENZYME-MIMIC PEPTIDE ASSEMBLY TO REALIZE AMIDOLYTIC ACTIVITY	69
4.1 Introduction	69
4.2 Materials and Methods	70
4.2.1 Peptide Synthesis	70

4.2.2	Fibril Sample Preparation	71
4.2.3	Amidolytic Activity Measurement	71
4.2.4	Inhibition Assay	72
4.2.5	Circular Dichroism (CD) Spectroscopy	73
4.2.6	Atomic Force Microscope (AFM)	73
4.2.7	Congo Red Staining	73
4.2.8	Raman Spectroscopy	74
4.2.9	Wide-Angle X-ray Scattering (WAXS)	75
4.3	Results and Discussion	75
4.3.1	Concept and Design	75
4.3.2	Structural Characterization of PCs Under pH Effect	77
4.3.3	Congo Red Staining to Observe the Amyloid-like Fibrils	85
4.3.4	Amydolytic Activity of Self-Assembled PC: pH Effect	88
4.3.5	Amydolytic Activity of Self-Assembled PC: Concentration Effect	92
4.3.6	Amydolytic Activity of Self-Assembled PC: Temperature Effect	93
4.3.7	Substrate Specificity Study	98
4.3.8	Inhibition Assay	100
4.3.9	Proposed Calculation of Rate Constant, k Involved the Catalytic Site Number of PC.	102
	CHAPTER FIVE: CONCLUSION	108
	REFERENCES	110
	APPENDICES	
	LIST OF PUBLICATIONS AND CONFERENCES	

LIST OF TABLES

	Page
Table 3.1 Physical properties of NMGs.	40
Table 3.2 Catalytic constants of NMG–10% 1-VI and NMG–10% DMAPM at different pH.	47
Table 3.3 Comparison of catalytic constants between different concentrations of 1-VI functional groups incorporated into NMG.	52
Table 3.4 Catalytic constants of NMG–20% 1-VI (ζ -potential is 22.5 ± 3.8 mV at 25 °C) with different mono peptide and oligopeptide/protein substrates.	55
Table 3.5 Distance between functional group of the NMG based on the proposed theoretical average distance.	62
Table 3.6 Debye-Huckel length of NMGs.	63
Table 4.1 Amino acid sequences of the designed PCs.	76
Table 4.2 Analyses of the secondary structures of PCs from the CD data.	79

LIST OF FIGURES

		Page
Figure 2.1	Simplified representation of the proteases specificity according to Schechter and Berger. The amino acid residues of the substrate are denoted by P and P', respectively. They interact with the corresponding S and S' subsites of the enzyme active site, respectively. The arrow indicates the site of hydrolytic cleavage.	6
Figure 2.2	Schematic illustration of the proteolytic action of serine proteases (α -chymotrypsin numbering).	8
Figure 2.3	Proteases are classified into four main mechanistic classes: (a) serine, (b) cysteine, (c) aspartic, (d) and metalloproteases. In the image, the pale blue curve in (a) and (b) represent oxyanion holes; the large curves with different colors represent the enzyme schematically. Red arrows indicate movement of electron pairs. Blue dotted lines represent hydrogen bonds or other electrostatic interactions. Grey lines represent the continuation of the substrate polypeptide to either side of the peptide bond.	10
Figure 2.4	A schematic illustration of proteases having both forward reaction (hydrolysis) and backward reaction (aminolysis). The areas that shaded in red color indicate the position of amide bonds in a short polypeptide.	13
Figure 2.5	The peptide synthesis chemistry had started to gain attention followed by the chemical approach via (a) the solid-phase peptide synthesis (SPPS). Owing to the aminolysis feature of proteases, protease-mediated polypeptide synthesis has become more valuable tool in peptide synthesis chemistry through (b) a thermodynamically controlled synthesis (TCS) or (c) a kinetically controlled synthesis (KCS).	15

Figure 2.6	A brief timeline for the development of artificial catalysts up to year 2000. The first attempt of mimic was done on cyclodextrin with the incorporation of imidazole rings. More sophisticated designs of cyclodextrin were then introduced when 3D structures of hydrolytic enzymes such as lysozyme and α -chymotrypsin were discovered. Other artificial catalysts also including macromolecular scaffold like crown ether, as well as peptide-based mimic like cyclic peptide.	18
Figure 2.7	(a) Chemical structure and (b) volume phase transition of NIPAm-based microgel at temperature below and above the lower critical solvent temperature, LCST (*LCST is typically around 30–40°C).	23
Figure 2.8	Schematic illustrations showing (a) temperature-responsive pK_a shift of proton-imprinted nanoparticles triggered by the phase transition and (b) the “catch and release” lysozyme purification from egg whites.	25
Figure 2.9	Schematic illustration of the imprinting of specific cavities in a cross-linked polymer by a template (T) with three different binding groups.	27
Figure 2.10	Typical examples of secondary structure-liked peptide-based artificial catalysts. (a) A four helix bundle or “chymohelizyme” that mimicked the catalytic activity of α -chymotrypsin and (b) A modeled structure of helix-loop-helix motif showing the positions of all incorporated histidine residues.	29
Figure 2.11	Schematic illustration of amyloid fibers. They are composed of rich β -sheet secondary structures that are oriented anti-parallelly and perpendicularly to the fibril axis.	30
Figure 3.1	Chemical structures of synthesized microgels.	35
Figure 3.2	A schematic illustration of amidolytic activity measurement of p(NIPAm)-based microgels hydrolyzing <i>p</i> -nitroaniline-based	37

	substrate through colorimetric assay.	
Figure 3.3	^{13}C NMR of NMG–20% 1-VI in D_2O .	41
Figure 3.4	(a) Spectrum analysis for amidase activity of NMG–10% 1-VI at 40 g/L. Amidase activity on substrate, L-alanine <i>p</i> -nitroanilide (0.25 mM) using different concentrations of three different NMGs (b) NMG–10% 1-VI, (c) NMG–10% DMAPM, (d) NMG–10% APM at 25°C, pH 8. All data shown are the means of triplicate tests, and mean data accompanied by asterisks are significantly different (Tukey's HSD test, $p < 0.05$).	43
Figure 3.5	Esterase activity on substrate, <i>p</i> -nitrophenyl acetate using 40 g/L of NMG–1-VI 20% at 25°C, pH 8. (a) Amount of <i>p</i> -nitrophenol released as a function of time. Reaction rate of each concentration of substrate, r was obtained through the slope. (b) Reaction rates obtained were then plotted as a function of substrate concentration and the rate constant, k was determined through the slope of the graph. All data shown are the means of triplicate tests.	45
Figure 3.6	(a) Acid–base titration of polymer catalyst solution of NMG–5% 1-VI (blue), NMG–10% 1-VI (green), NMG–15% 1-VI (red), NMG–20% 1-VI (purple), and NMG–10% DMAPM (black) at 25°C against HCl. (b) The fraction of protonated functional group for different NMGs.	49
Figure 3.7	Amidase activity on substrate, L-alanine <i>p</i> -nitroanilide (0.25 mM) using ionized NMG–10% DMAPM and NMG–10% DMAPM (as control) at 25°C, pH 8. All data shown are the means of triplicate tests, and mean data accompanied by asterisks are significantly different (Tukey's HSD test, $p < 0.05$).	51
Figure 3.8	The influence of temperature on the amidase activity on substrate, L-alanine <i>p</i> -nitroanilide using 40 g/L of NMG–1-VI	53

20% at pH 6. Insets show the transition of NMG from swollen state (25°C) to shrunken state as the temperature increased to 50°C. All data shown are the means of triplicate tests.

- Figure 3.9 A schematic illustration of proposed amidase activity mechanism for NMG-1-VI with repeating steps of (a) Protonation of 1-VI, (b) Nucleophilic attack of hydroxide ion, and (c) Substrate was cleaved into R'-NH₂ and R-COOH as products, whereby R'-NH₂ represents released chromophore, *p*-nitroaniline in this study. 59
- Figure 3.10 (a) A schematic diagram of proposed theoretical average distance from the radius of a sphere. The volume occupied per functional group is assumed in a sphere and the functional group is at the center of a sphere. The calculated distance is assumed to be $2r$. (b) Relationship between catalytic rate and calculated distance. Turnover rate for α -chymotrypsin was taken from the reported result as mono-peptide-*p*-nitroanilide substrates were used. The inset displays the enlarged area for NMG with different concentrations of 1-VI. 61
- Figure 3.11 Linear plot of the relationship between catalytic rate and calculated distance. Turnover rate for α -chymotrypsin was taken from the reported result as mono-peptide-*p*-nitroanilide substrates were used. 65
- Figure 3.12 Dixon plots of NMG-20% 1-VI with different types of inhibitors (a) UV, (b) PMSF and (c) E-64 using L-alanine *p*-nitroanilide as substrate at 25°C, pH 6. The Dixon plots here were used to calculate the inhibitor constant, K_i of the NMG. According to the Dixon method, K_i is determined when the straight lines generated from different substrate concentrations intercept each other at a point on the left of the vertical axis. Therefore, the value of $-K_i$ can be determined directly. 68
- Figure 4.1 CD spectra of different PCs fibrillated at different pH and collected at the time point of 96 h in 25°C: (a) PC1, (b) PC2, 78

	(c) PC3, (d) PC4, (e) PC5, and (f) PC6. Peptide concentration was fixed at 10 μ M in all conditions.	
Figure 4.2	AFM images of different PCs fibrillated at different pH and taken at the time point of 96 h in 25°C; scale bar: 1 μ m.	80
Figure 4.3	The size distributions of PC3 in terms of width, height, and length of fibrillated fibers at different pH with different incubation times. All data shown are the means of replicate tests ($n = 30$), and mean data accompanied by asterisks (*) are significantly different (Tukey's HSD test; $p < 0.05$).	82
Figure 4.4	The size distributions of PC4 in terms of width, height, and length of fibrillated fibers at different pH with different incubation times. All data shown are the means of replicate tests ($n = 30$), and mean data accompanied by asterisks (*) are significantly different (Tukey's HSD test; $p < 0.05$).	83
Figure 4.5	Microscopic and spectroscopic analyses of Congo red staining. Interactions of Congo red with (a) PC3 and (b) PC4 that incubated at different pH were seen with the presence of green birefringence coming from the regions rich in β -sheet fibrils; scale bar: 10 μ m. (c) The UV-Vis spectra of PC3 and PC4 stained with Congo red. A maximal spectral difference at 540 nm indicates the presence of amyloid-like fibrils.	86
Figure 4.6	Optical microscope images of <i>Bombyx mori</i> silk as positive control, were taken under cross-polarized light stained with Congo red. (a) <i>B. mori</i> showed green birefringence coming from regions rich in β -sheet structures. (b) Non-polarized images of <i>B. mori</i> ; scale bar: 20 μ m.	87
Figure 4.7	Amidolytic activity on substrate, L-alanine <i>p</i> -nitroanilide (0.25 mM) of (a) PC4 and (b) PC3, after 96 hours of fibrillation at different pH. The final reaction was done using 0.1M Tris-HCl buffer at pH 8 and 25°C. (c) Amidolytic activity of PC4 at different pH. All data shown are the means of triplicate tests,	89

	and mean data accompanied by asterisks (*) are significantly different (Tukey's HSD test; $p < 0.05$).	
Figure 4.8	(a) The PC solution became viscous and transparent when the incubation pH increased from pH 8 to pH 10 and 12. (b) Amidase activity on substrate, L-alanine <i>p</i> -nitroanilide (0.25 mM) using soluble fibers of PC4 at 25°C, pH 8 to confirm the less active soluble form of PC4. All data shown are the means of triplicate tests.	91
Figure 4.9	Amidase activity on substrate, L-alanine <i>p</i> -nitroanilide (0.25 mM) using different concentrations of PC4 at 25°C, pH 8. All data shown are the means of triplicate tests, and mean data accompanied by asterisks (*) are significantly different (Tukey's HSD test, $p < 0.05$).	93
Figure 4.10	The effects of temperature on fibrillation of PC4 were evaluated. AFM images of PC4 incubated at different temperatures until a stable formation (based on the size distribution of PC4 over time) of fibrils at a specific time point: (a) after 96 h of incubation at 25°C, (b) after 48 h of incubation at 50°C, and (c) after 24 h of incubation at 70°C; scale bar: 1 μm. (d) CD spectra demonstrate the predominant of β-strand structure of PC4 at respective time points of different temperatures. (e) Amidase activity on substrate, L-alanine <i>p</i> -nitroanilide (0.25 mM) of 2 mM of PC4, after respective fibrillation durations at different temperatures. The final reaction was done at 25 °C. All data shown are the means of triplicate tests, and mean data accompanied by asterisks (*) are significantly different (Tukey's HSD test; $p < 0.05$).	94
Figure 4.11	CD spectra of PC4 fibrillated at (a) 50°C and (b) 70°C with different time points.	95
Figure 4.12	(a) AFM images of PC4 fibrillated at different temperature and taken at different time points in 25°C; scale bar: 1 μm. The size distributions of PC4 fibrillated at (b) 50°C and (c) 70°C in	97

terms of width, height, and length of fibrillated fibers at different pH with different incubation times. All data shown are the means of replicate tests ($n = 30$), and mean data accompanied by asterisks (*) are significantly different (Tukey's HSD test; $p < 0.05$).

- Figure 4.13 Amidase activity on different types of substrate (fixed concentration at 0.25 mM) of 2 mM of PC4 after 4 days of incubation at pH 8 and 25 °C. All data shown are the means of triplicate tests, and mean data accompanied by asterisks (*) are significantly different (Tukey's HSD test; $p < 0.05$). 98
- Figure 4.14 Inhibition assay on different concentrations of inhibitors (a) PMSF and (b) APMSF after 4 days of incubation at pH 8 and 25 °C. All data shown are the means of triplicate tests. 101
- Figure 4.15 Schematic illustration showing the structural model of PC4 and how it might pack and laminate to form fibrils observed from the atomic-level information. (a) Raman spectrum of PC4 with the main assignments including, amide I and III. (b) X-ray diffraction pattern of PC4 showing the reflections that define the packing and orientation of fibers. (c) Short peptide arrangements of PC4 from β -strands to β -sheets and unit cell dimensions, which in consistent with various characterizations (a is the hydrogen bonding distance along the fiber axis, c is the peptide length, and b is the intersheet spacing). 103
- Figure 4.16 Amidase activity on different concentrations of substrates, L-alanine-*p*-nitroanilide using 2 mM of PC4 at 25°C, pH 8. (a) Amount of *p*-nitroaniline released as a function of time. Reaction rate of each concentration of substrate, r was obtained through the slope. (b) Reaction rates obtained were then plotted as a function of substrate concentration and the rate constant, k was determined through the slope of the graph. All data shown are the means of triplicate tests. 106

LIST OF ABBREVIATIONS

1-VI	1-vinylimidazole
1D	One-dimensional
2D	Two-dimensional
3D	Three-dimensional
AAPD	2,2'-azobis(2-methylpropionamidine)dihydrochloride
AFM	Atomic force microscope
Ala	Alanine
APM	<i>N</i> -(3-aminopropyl)methacrylamide
APMSF	<i>p</i> (4)-amidinophenylmethanesulfonyl fluoride
Arg	Arginine
Asp	Aspartic acid
BIS	<i>N,N'</i> -methylenebisacrylamide
CD	Circular dichroism
Co	Cobalt
CR	Congo red
CTAB	Cetyltrimethylammonium bromide
Cys	Cysteine
DLS	Dynamic light scattering
DMAPM	<i>N</i> -[3-(dimethylamino)propyl]methacrylamide
E-64	<i>N</i> -[<i>N</i> -(<i>L</i> -3-transcarboxyirane-2-carbonyl)- <i>L</i> -leucyl]-agmatine
FITC	Fluorescein thiocarbonyl
FPD	Flat-panel detector
Gln	Glutamine
Gly	Glycine
His	Histidine
HPLC	High-performance liquid chromatography
KCS	Kinetically controlled synthesis
LCST	Lower critical solvent temperature
Leu	Leucine
MALDI-TOF	Matrix-assisted laser desorption/ionization-time of flight mass

	spectrometry
Mg	Magnesium
MWCO	Molecular weight cut off
NaDBS	Sodium dodecylbenzene sulfonate
NIPAm	<i>N</i> -isopropylacrylamide
NMG	NIPAm microgel
NMG–1-VI	NMG bearing functional group of 1-VI
NMG–APM	NMG bearing functional group of APM
NMG–DMAPM	NMG bearing functional group of DMAPM
NMR	Nuclear magnetic resonance
NPs	NIPAm nanoparticles
P(NIPAm)	Poly(<i>N</i> -isopropylacrylamide)
PC	Peptide catalyst
PEEK	Poly(etheretherketone)
Phe	Phenylalanine
PMSF	Phenylmethanesulfonyl fluoride
PNPA	<i>p</i> -nitrophenyl acetate
Pro	Proline
RNase	Ribonuclease
SDS	Sodium dodecyl sulfate
Ser	Serine
SPPS	Solid-phase peptide synthesis
TCS	Thermodynamically controlled synthesis
Thr	Threonine
Trp	Trypsin
Tyr	Tyrosine
UV	Uridine vanadate
Val	Valine
WAXS	Wide-angle x-ray scattering
Zn	Zinc

REKA BENTUK DAN PENILAIAN PEMANGKIN BUATAN YANG MEMPUNYAI PEMANGKINAN AMIDASE MIRIP ENZIM

ABSTRAK

Kajian ini dijalankan bertujuan untuk mengkaji kebolehan dan pengesahan reka bentuk pemangkin buatan baru yang diperbuat dengan konsep pemangkin buatan polimer dan pemangkin buatan peptida. Beberapa jenis ujian penilaian telah dilakukan atas reka bentuk pemangkin buatan baru untuk memastikan keupayaan mereka menjalankan pemangkinan amidase mirip enzim. Keupayaan mikrogelpoli(*N*-isopropilakrilamida) (NMG) telah dikembangkan dengan penambahan pelbagai kumpulan berfungsi untuk mengawal caj permukaan, hidrofobisiti, pK_a dan kapasiti penjerapan protein, tetapi mikrogel masih kurang dilibatkan dalam perekaan pemangkin buatan. Dalam kajian ini, NMG yang telah direkapipta dengan tiga jenis kumpulan berfungsi sebagai pemangkin buatan polimer, digunakan untuk mengurai ikatan amida. Pelbagai strategi penilaian telah diuji untuk aktiviti penguraian yang cekap ke atas substrat *p*-nitroanilina dengan menggunakan ujian kolorimetri. Berdasarkan keputusan yang diperolehi, satu mekanisme untuk menguraikan ikatan amida dan menentukan jarak purata teori antara kumpulan berfungsi telah dicadangkan dengan menggunakan NMG yang ditambahkan kumpulan berfungsi 1-vinylimidazol sebagai model kajian. Hidrolisis kumpulan amida telah direncatkan apabila perencat protease peringkat transisi digunakan, telah mengesahkan model tindak balas yang dicadangkan untuk NMG. Keputusan yang diperolehi memberikan pemahaman atas perkembangan strategi untuk merekapipta hidrogels yang berfungsi sebagai pemangkin buatan. Pemangkin buatan tersebut

berpotensi untuk digunakan dalam reaksi penukaran secara biologi dan kimia serta dalam penggunaan terapi perubatan. Bahagian seterusnya melaporkan satu lagi reka bentuk pemangkin buatan jenis peptida berdasarkan stuktur gentian amiloid. Gentian amiloid telah dikelaskan sebagai bahan nano generasi baru disebabkan oleh cirinya seperti kesejagatan, daya talaan, dan kekakuan. Di sini, pemangkin protease serine telah diperkenalkan ke dalam reka bentuk urutan peptida pendek melalui pendekatan pemangkin buatan baru mirip protease. Penghasilan polimorf gentian daripada peptida pendek yang diperhatikan pada pH dan suhu yang berbeza telah memberikan kemungkinan untuk menghasilkan struktur gentian yang juga berbeza. Struktur gentian tersebut dipercayai akan menjejaskan kecekapan aktiviti penguraian pemangkin buatan peptida (PC). Berdasarkan keputusan yang diperolehi daripada AFM, spektroskopi Raman, dan WAXS, model struktur gentian telah dibincangkan dan dikaitkan dengan bilangan tapak pemangkinan pengiraan kadar perolehan PC. Keputusan yang diperolehi daripada PC setakat ini juga memberikan pemahaman atas potensinya sebagai pemangkin buatan peptida yang cekap dan penyiasatan struktur secara mendalam melalui cara dinamik molekul adalah diperlukan.

DESIGN AND EVALUATION OF ARTIFICIAL CATALYSTS THAT POSSESS ENZYME-LIKE AMIDOLYTIC CATALYSIS

ABSTRACT

In the present study, with the main goal of mimicking the amidase activity of protease, artificial polymer catalyst and peptide catalyst were designed and synthesized followed by various evaluations to investigate the validity of the design to possess enzyme-like amidolytic catalysis. Poly(*N*-isopropylacrylamide) microgel (NMG) has been developed by adding various functional groups to control surface charges, hydrophobicity, pK_a and protein adsorption capacity but seldom for enzyme mimics. Here, NMGs anchored with three types of functional groups were developed and studied as polymer catalysts to hydrolyze amide bonds under evaluated mild conditions. Various evaluation strategies were tested for efficient hydrolysis activity on a *p*-nitroaniline-based substrate by using a colorimetric assay. Based on the results, a mechanism was proposed to hydrolyze amide bonds and determine the theoretical average distance, using NMG bearing functional group of 1-vinylimidazole as the study model. The hydrolysis of amide bonds was inhibited by a transition-state protease inhibitor, which also confirmed the proposed reaction model for NMG. These results provide an insight into the strategies developed to functionalize hydrogels through an enzyme-mimic approach for future robust bio- and chemical conversions as well as therapeutic utilities. The next part of this study reported another artificial catalyst design in the form of peptide catalyst based on amyloid fibers structure. Amyloid fibers have classified as new generation of tunable bio-nanomaterials with new functions due to the distinctive characteristics of

amyloid fibers such as universality, tunability, and stiffness. Here, catalytic residues of serine protease were introduced into the peptide sequences of short peptides design through an enzyme-mimic approach. The observation of distinct polymorphs involving the manipulation of fibrillation of short peptides at different pH and temperatures, highlights the possibility for generating different fibril packing, and hence greatly affect the amidolytic activity of peptide catalyst (PC). Based on the results from AFM, Raman spectroscopy, and WAXS, the fibril structural model was discussed and correlated to the catalytic site number for turnover rate calculation of PC. These results provide insight into the potential of designed PC to form efficient artificial catalysts for amidolytic activities and also indicate a necessary future work regarding the investigation of catalytic triads' side chain conformation through molecular dynamics.

CHAPTER ONE

Introduction

1.1 General Introduction

The chemistry that is inspired by biological processes is termed as “biomimetic chemistry” in 1972 by Ronald Breslow (Breslow, 1972; Breslow, 2009). Biomimetic chemistry involves a wide area of studies that include the study of artificial catalysts (Breslow & Dong, 1998), the study of self-assembly of small molecules (He et al., 2009) and the study of biological model for the synthesis of natural products (Nicolaou et al., 2003). In the field of biomimetic chemistry, the main idea is to create and develop a new chemical catalysis and processes from the key principles and concepts used in biological systems. The study of artificial catalysts in particular, has developed rapidly by fully exploiting this idea since 1970s. The inspiration for a new design of artificial catalyst can come from the functions and structures of natural compounds. The chemical reactions that occur on the natural world are almost representing the reactions of life. Hence, it is not surprising that researchers have been interested in mimicking and generalizing the biochemical reactions of nature. Since enzymes or catalysts have been playing the crucial role in catalyzing most of the chemical reactions, numerous works have been done to produce a promising artificial catalyst.

In order to be useful as an artificial catalyst, especially an industrial catalyst, broad substrate specificity is preferred to create an ideal and efficient catalyst which would have the ability to perform all the general biochemical reactions (Breslow, 1982; Kirby, 1996). However, the high catalytic efficiency of natural enzymes is strongly related to the geometric control by the enzyme, so that the biochemical

reactions are happened in a way that the catalytic groups are held nearby with a particular spatial arrangement for an effective interaction with the bound substrate molecules. Therefore, for many practical purposes, it is more crucial to mimic the selectivity of enzyme-catalyzed reaction than to solely achieve their velocity. The achievement of good selectivity has been a major objective for the study of artificial catalysts.

In the present study, with the main goal of mimicking the catalytic action of protease (*e.g.* α -chymotrypsin), the amidase activity, poly(*N*-isopropylacrylamide) was chosen as a potential candidate to be the major part of one of the artificial catalyst designs as polymeric catalyst. “Smart” polymer which possesses the ability to respond to different environments, such as temperature, buffer, and pH, provides an element of remote controllability. The successful design of this type of polymer catalyst could enable an interesting controllability of acceleration or deceleration of the catalytic rate, corresponding to the reaction environment in which it is situated. The development of artificial catalysts for the specific aforementioned geometric control and spatial arrangement would require another artificial catalyst design with complementing qualities. The formation of β -sheet structure through the self-assembly of short peptides in the form of fibrils was hypothesized to be the key point of this new design since it endowed with a closer and stable binding sites as well as catalytic sites due to the regular spacing of β -sheet structure in fibril. Therefore, the conformational stability of peptide catalyst design could provide a structural framework support for efficient catalytic activities.

As future perspectives, with improved and more sophisticated design of polymeric catalyst and peptide catalyst with better mimic of protease, they would catalyze peptide synthesis. Protease-mediated polypeptide synthesis proceeds

through either a thermodynamically controlled synthesis (TCS) or a kinetically controlled synthesis (KCS). TCS is a reversal of hydrolysis and requires conditions, which shift the equilibrium towards synthesis of polypeptides. Polypeptides have been coined as ‘next’-generation, which could be used in the production of new biomaterials for gene and drug delivery, biomedical imaging and so on (Baker & Numata, 2013).

1.2 Hypothesis and Aims of Thesis

This thesis focused on the design of artificial catalysts that mimicked the catalytic action of protease, the amidase activity. The “smart” polymer, poly(*N*-isopropylacrylamide) and regular spacing of β -sheet structure in fibril structure have shown attractive features to meet the important requirement of geometric control and spatial arrangement for effective artificial catalyst design. Evaluation of artificial catalysts in terms of concentrations, pH, temperature and so on are important for understanding the structural stability of designed artificial catalysts as well as to observe the relationship between the change of microenvironment under different study parameters and catalytic efficiency.

Specific aims of thesis were:

1. To design the artificial catalysts that mimicked the amidase activity of enzyme protease.
2. To explore the capability of designed artificial catalysts to possess enzyme-like amidolytic activity through various study parameters.
3. To elucidate the mode of catalytic action of artificial catalysts based on the structural postulation around the catalytic “pocket”.

CHAPTER TWO

Literature Review

2.1 Native Enzymes and Its Mechanisms

As known, enzymes play a biologically crucial role in catalyzing chemical reaction with high efficiency and selectivity in living systems from their unique catalytic microenvironments (Schramm, 1998). Enzymes are magnificent biological catalysts with the capability to accelerate the rate of chemical reactions up to 10^{19} times for specific substrates and reactions (Wolfenden & Snider, 2001). The crucial role of enzymes in the life processes is reflected in the fact that enzymes possess several interesting characteristics for example, the optimum rate of enzymes is mostly at mild conditions or physiological pH and temperature, needed in small amount and reusable, and their reactions, where necessary, are fully chemo-, regio- and stereoselective (Walsh, 2001). Enzymes can be roughly categorized into two major groups, functional group enzymes or metalloenzymes. The catalysis reactions of functional group enzymes involve only the side chains of the polypeptide backbone of the enzyme, while metalloenzymes use additional metal-ions for catalytic purposes via the immobilization of those metal-ions to the functional groups of the enzymes. Since proteases are the major target for enzyme mimic in this project, more details about proteases only will be discussed in the following sections.

2.1.1 Proteases

Proteolytic enzymes or proteases selectively catalyze the hydrolysis of peptide bonds and they are divided into four major classes: aspartic protease, serine protease, cysteine protease, and metalloprotease. Proteases play important roles in our daily lives as laundry detergents to help remove protein-based stains and meat

tenderizers, as well as several important physiological processes including digestion, blood coagulation, fertilization, cell differentiation and growth. Proteases are also useful for various drug tests as targets, teaching models for introductory enzymology and important component in molecular biologist's tool kit (Southan, 2001).

In general, proteases differ in the specificities that they behave during the hydrolysis reactions and their specificity is determined by the catalytic triad at the active site. This fact is further proven based on the analysis of three-dimensional structures using X-ray crystallography (Bommarius & Riebel, 2005). Proteases usually contain a channel or a "pocket" on their surface that near to the active site, which binds specifically to the amino acid side chains of the polypeptide substrate. Due to different interactions in this region there are great differences in the so-called primary specificity of the proteases. For instance, trypsin hydrolyses only those substrates contain the peptide bonds adjacent to the amino acids of lysine or arginine, which are positively charged and hydrophilic. On the other hand, a negatively charged aspartic acid unit is situated at the back of the binding pocket of trypsin, holding the positively charged lysine or arginine side chain through electrostatic forces. From the above example, the aspartic acid is obviously important for binding, however, it is not the only binding site and it is believed that the binding of substrates involves interactions at a number of subsites on either side of the pair of residues having the peptide bond to be hydrolyzed. An optimal configuration is necessarily to be oriented at the active site by fixing the enzyme and substrate at several important points (Breslow et al., 2006).

Based on the idea above, a system of nomenclature to describe the interaction of proteases and their substrates was introduced in 1967 by Schechter and Berger (Schechter & Berger, 1967). They suggested numbering the different regions within

the binding pocket according to the amino acid residues that bind there as a series of subsites S and the distance of these amino acids from the amino acid building blocks P of the peptide or protein substrate to be hydrolyzed (Figure 2.1).

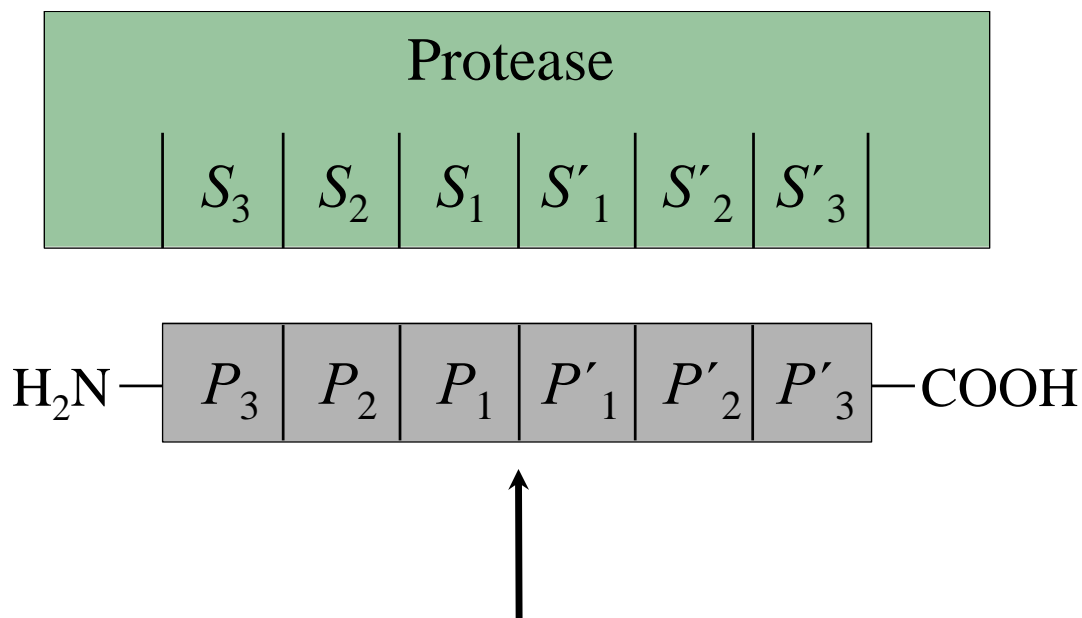


Figure 2.1 Simplified representation of the proteases specificity according to Schechter and Berger. The amino acid residues of the substrate are denoted by P and P' , respectively. They interact with the corresponding S and S' subsites of the enzyme active site, respectively. The arrow indicates the site of hydrolytic cleavage.

The amino acid residues of the substrate are denoted by P and P' , respectively, which interact with the corresponding S and S' subsites within the active site of the proteases. The acyl part of the peptide bond to be cleaved lies in the $S_1 \dots S_n$ binding sites, while the amino part of the peptide bond to be cleaved lies in the $S'_1 \dots S'_n$ binding sites. The substrate residues are called $P_1 \dots P_n$ and $P'_1 \dots P'_n$ according to their location relative to the amide link being hydrolyzed, shown as the arrow in Figure 2.1. Detailed mapping of the active sites has given a better understanding of the relationship between substrate and proteases and has enlightened both the design and synthesis of artificial enzymes as well as a prediction of the outcome of the reverse reaction of protease in polypeptides synthesis (see Section 2.1.1.5).

The overall process of proteolytic action is identical in all classes of proteases (serine, cysteine, aspartic and metalloproteases) but differ in the groups that perform the nucleophilic attack, general base catalysis, and electrophilic assistance. The proteolytic action starts with the attack on the carbonyl group of the peptide bond, which requires a nucleophilic agent (normally oxygen or sulfur), as a means to approach the slightly electrophilic carbonyl carbon atom. A proton is then removed from the attacking nucleophile with the assistance of general base catalysis (Dunn, 1989). Different proteases also differ in the groups that involved in the breakdown of the tetrahedral intermediate which is formed in the initial nucleophilic attack, expecting the departure of the amine fragment through general acid catalysis. The different catalytic mechanisms of four types of proteases were first revealed by the use of some group-specific inhibitors (Blow, 1976).

2.1.1(a) Serine Proteases

Serine proteases are the most studied class of proteases and the commonly found members are α -chymotrypsin, trypsin, and subtilisin (Barrett & Rawlings, 1995). The hydrolysis of peptide bond involves an acyl-enzyme intermediate in which the hydroxyl group of reactive serine residue, Ser¹⁹⁵ (from the α -chymotrypsin numbering system) is acylated by the acyl group of the substrate and amine moiety is released as well as the product. The amide hydrolysis mechanism (acid-base mechanism) at the active site of α -chymotrypsin was first proposed by Blow *et al.* in 1969, and was termed as 'charge relay system'. As shown in Figure 2.2, the main features of this system were acylation, in which an acyl-enzyme intermediate is formed through the transfer of the acyl group from the substrate to the enzyme after a nucleophilic attack from Ser¹⁹⁵. At the same time, the proton of the serine is

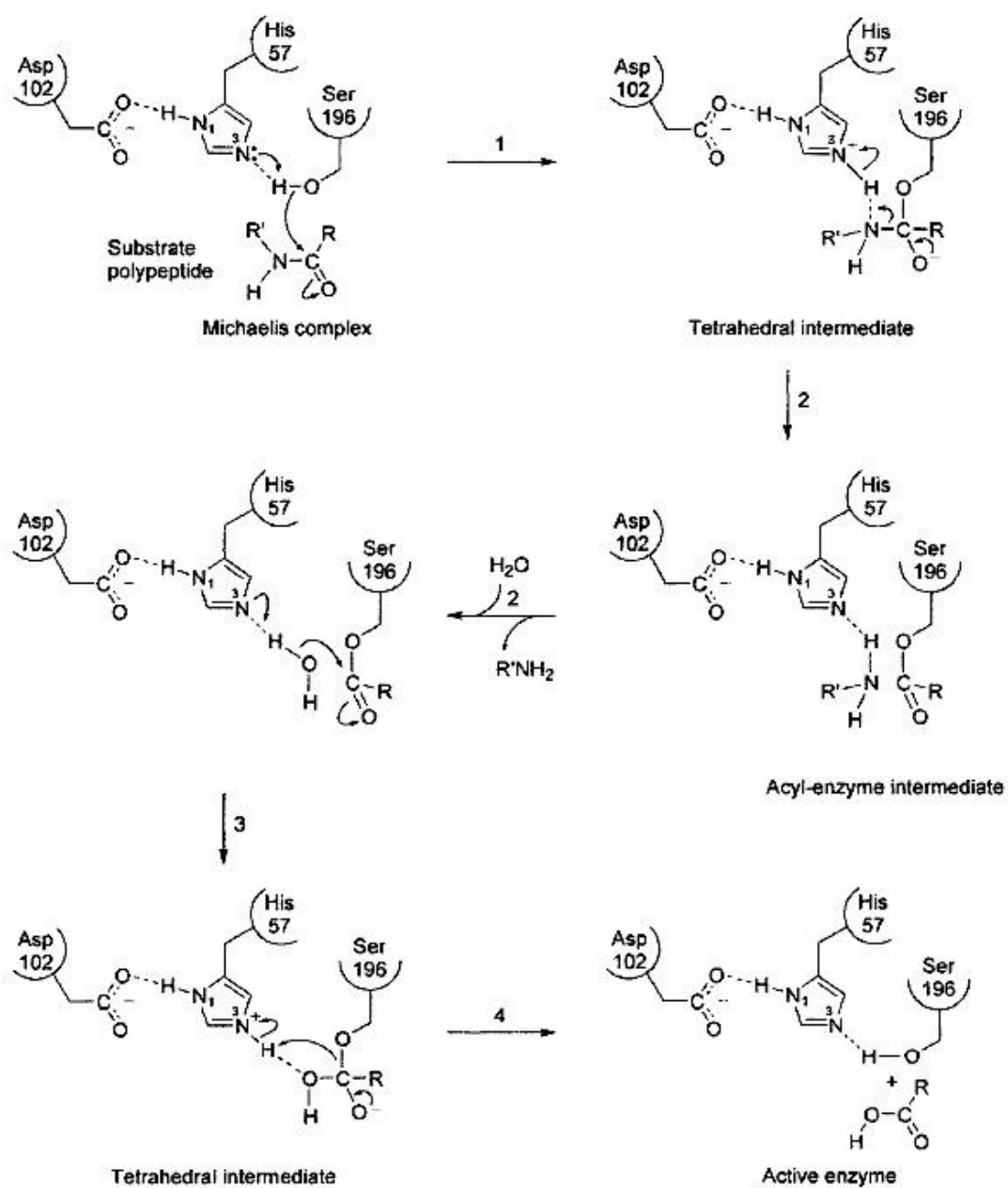


Figure 2.2 Schematic illustration of the proteolytic action of serine proteases (α -chymotrypsin numbering). Figures adapted from Jakubke (2002).

transferred to the histidine residue, His⁵⁷ thereby forming an imidazolium ion. This step was followed by deacylation, which involves the cleavage of the intermediate by water molecules and release of the product (Blow et al., 1969). Asp¹⁰² is playing a supporting role in this catalytic mechanism through the polarizing effect of itself in the form of carboxylate ion which is hydrogen bonded to His⁵⁷ in the sense of electrostatic catalysis. Apart from the catalytic residues, there is another feature which is equally notable in the whole process of proteolytic action, the oxyanion hole. The existence of oxyanion hole is important to stabilize frequently the tetrahedral intermediate via the interaction with several hydrogen bond donors. In this case, the resulting oxyanion hole is hydrogen-bonded to the backbone NH groups of Gly¹⁹³ and Ser¹⁹⁵ (Jakubke, 2002; Powers et al., 2002) (Figure 2.3a).

2.1.1(b) Cysteine Proteases

Cysteine proteases, also known as thiol proteases or sulfhydryl proteases, are commonly discovered in fruits, for example the archetypal cysteine protease, papain from papaya's latex (Kimmel & Smith, 1954) and bromelain from pineapple, as well as endopeptidases, like caspases. The catalytic mechanism of cysteine proteases is very identical to that of serine proteases in terms of using a strong nucleophile and the formation of a covalent enzyme-substrate complex in the process of proteolytic action. However, the attacking nucleophile is the thiol group of cysteine residue (Cys²⁵ in the papain numbering system), as opposed to the hydroxyl group of a serine as observed in serine proteases. Nevertheless, histidine residue (His¹⁵⁹) is still playing the same major role as a proton donor/general base in order to complete the whole process in cysteine proteases. Unlike serine proteases, an additional catalytic residue to orientate the imidazolium ring of the histidine residue is rather

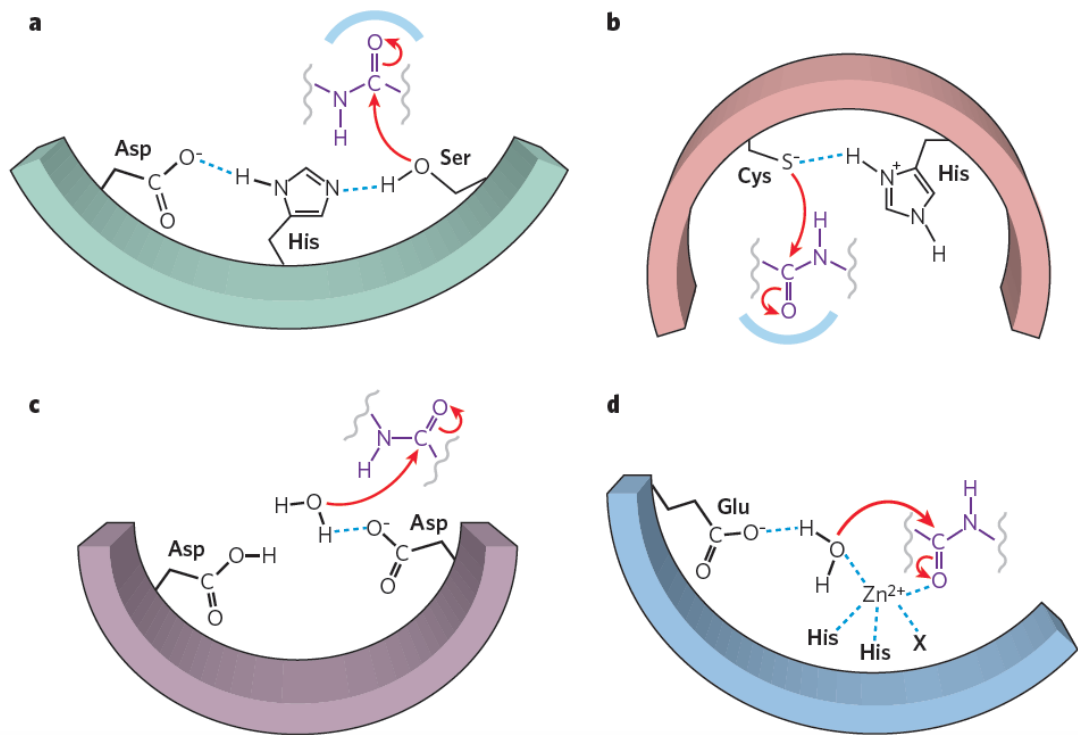


Figure 2.3 Proteases are classified into four main mechanistic classes: (a) serine, (b) cysteine, (c) aspartic, (d) and metalloproteases. In the image, the pale blue curve in (a) and (b) represent oxyanion holes; the large curves with different colors represent the enzyme schematically. Red arrows indicate movement of electron pairs. Blue dotted lines represent hydrogen bonds or other electrostatic interactions. Grey lines represent the continuation of the substrate polypeptide to either side of the peptide bond. Figures adapted from Erez et al. (2009).

unnecessary for cysteine proteases and catalytic dyad is more commonly encountered throughout the cysteine proteases' families. In the cysteine proteases papain, the backbone NH groups of Cys²⁵ and Gln¹⁹ form the oxyanion hole, which serves the same purpose as found in serine proteases to stabilize the tetrahedral intermediate (Harrison et al., 1997) (Figure 2.3b).

2.1.1(c) Aspartic Proteases

Aspartic proteases or aspartyl proteases have totally different catalytic mechanism as compared to serine and cysteine proteases. Instead of using the catalytic domain as the nucleophilic agent, activated water molecule plays the role as a nucleophile to attack the scissile peptide bond in this case. The water molecule coordinated between the main catalytic domains which consist of two aspartic acid side chains (Asp³² and Asp²¹⁵, as in pepsin numbering system), is activated by proton abstraction and followed by the nucleophilic attack of the water molecule on the carbonyl carbon of the substrate. Furthermore, no covalent tetrahedral intermediate could be formed between the enzyme and any moieties of the substrate due to two concurrent proton transfers which happen almost simultaneously in the formation and breakdown of the intermediate. The simultaneous proton transfers was coined as a “push-pull” general acid-base catalyzed nucleophilic attack (Polgár, 1987). The feature of oxyanion seems to be negligible too since the tetrahedral transition state formed on nucleophilic attack most likely is uncharged (Erez et al., 2009) (Figure 2.3c).

2.1.1(d) Metalloproteases

Metalloproteases possess almost the same attributes as aspartic proteases, which they do not form covalent intermediates and the nucleophilic attack on the peptide bond to be cleaved is assisted by a water molecule. However, metalloproteases are different in terms of activation of water molecule, which the activation is prompted by a divalent metal cation, often Zn^{2+} but sometimes also Co^{2+} or Mg^{2+} . The coordination number of the metal is accomplished by three histidine residues, or two histidine residues and an acidic side chain in many soluble metalloproteases, such as thermolysin and carboxypeptidase A. The water molecule is coordinated to the fourth tetrahedral site and this additional zinc ligand is often hydrogen-bonded to another supporting residue, glutamate, which abstracts a proton from the attacking water molecule. The oxyanion is present in metalloproteases and it is stabilized by the zinc ion itself (Sutton & Buckingham, 1987; McCall et al., 2000) (Figure 2.3d).

2.1.1(e) Protease-mediated Polypeptides Synthesis

Another unique feature of proteases that is worth to be attempted to mimic its enzymatic activity by chemists/enzymologists is the reverse reaction of proteases or aminolysis. Aminolysis or the synthesis of polypeptides is the formation of amide bonds between amino acid monomers by a condensation reaction between a carboxylic acid and an amine (Figure 2.4). Polypeptides have been coined as ‘next’-generation biomaterials that will have less toxic degradation products, undergo hierarchal assemble to form supramolecular structures, and maintain a sustainable design, as compared to synthetic polymers, which the degradation products of synthetic polymers are of acidic and cannot be metabolized biological systems, and

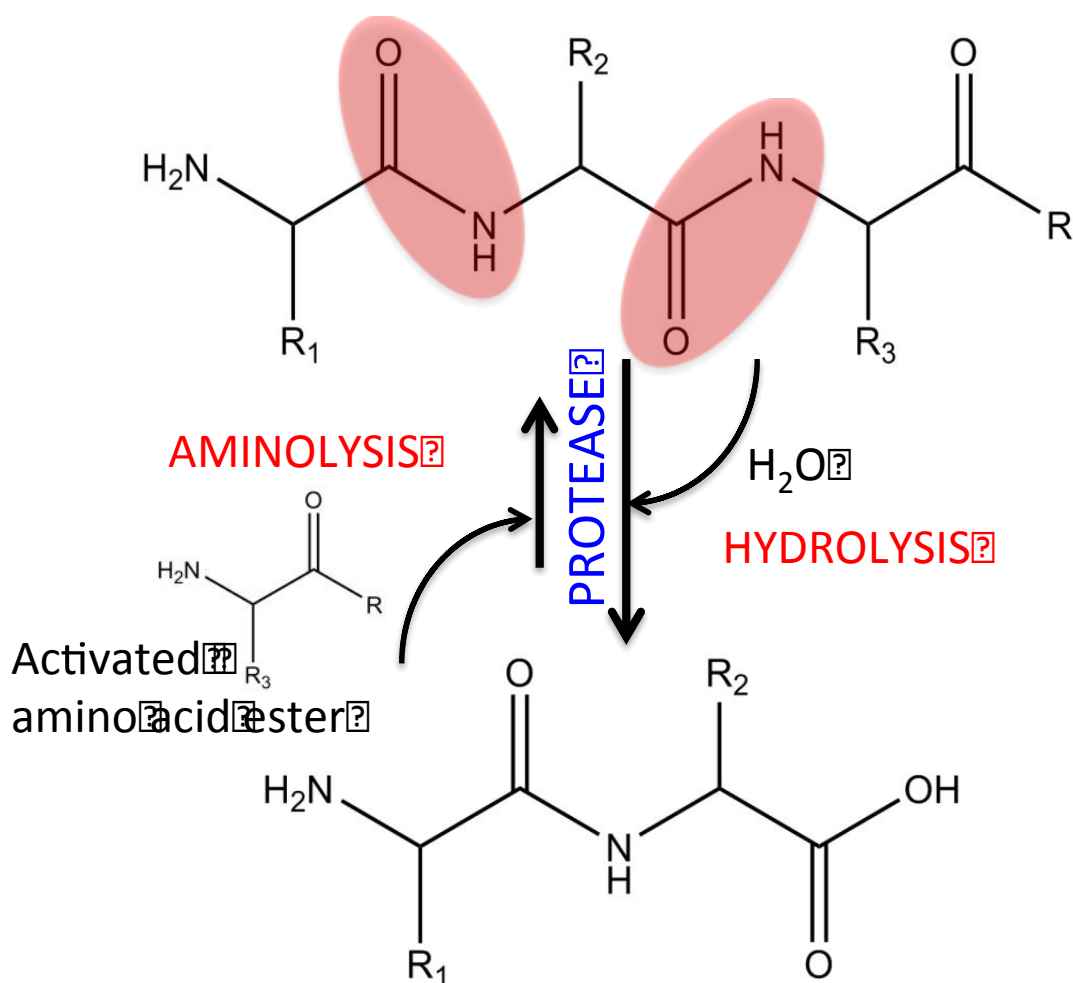


Figure 2.4 A schematic illustration of proteases having both forward reaction (hydrolysis) and backward reaction (aminolysis). The areas that shaded in red color indicate the position of amide bonds in a short polypeptide.

always reveal both environmental and sustainability concerns. Polypeptides have been given more attention nowadays and it becomes increasingly important class of bioactive compounds in enormous fields including physiology, biochemistry, medicinal chemistry, and pharmacology as hormones, neurotransmitters, cytokines, growth factors, and so on (Kim & Chaikof, 2010; Dai et al., 2011).

The origins of peptide synthesis chemistry are usually traced back to the conventional chemical method for amide bond where the activation of the carboxyl group is necessary to attract a nucleophilic attack by a free amine. This chemical reaction is usually coupled with the presence of coupling agents, base and solvents. The classical chemical peptide synthesis is solid-phase peptide synthesis (SPPS),

developed by the Noble laureate Bruce Merrifield. In SPPS, the amine group is protected and the N-terminal amino acid is attached to a matrix with the carboxyl group. This is followed by a deprotection step on the amine group in order to reveal an N-terminal amine for the subsequent coupling reaction between the activated carboxyl group of the next monomer and the amine group of the immobilized residue (Baker & Numata, 2013) (Figure 2.5a). It is also crucial to protect the side chains of several amino acids that containing functional groups, which may interfere the amide bond formation (Merrifield, 1964). However, SPPS is a time-consuming operation with complicated protection-deprotection steps and all the intermediates products have to be treated and characterized after each reaction step. Racemization is normally unavoidable too in SPPS.

Owing to the aminolysis feature of proteases, they have become valuable tools in synthetic organic chemistry due to the fact that proteases do not usually need cofactors or coupling agents during their catalytic function and the synthesized products are saved from racemization with maximum optical purity. Peptide synthesis catalyzed by proteases was first postulated by van't Hoff in 1898. Nevertheless, this speculation was proven only 40 years later in 1938 by Bergman and co-workers after a successful demonstration of protease-mediated synthesis of Leu-Leu and Leu-Gly dipeptides (Bergmann & Fruton, 1937, 1938). There are two types of protease-mediated polypeptide syntheses, a thermodynamically controlled synthesis (TCS) or a kinetically controlled synthesis (KCS). TCS or the equilibrium-controlled represents a reversal of hydrolysis and conditions are required to shift the equilibrium towards synthesis. Those conditions include addition of water-miscible organic solvents, acidity reduction of the carboxyl group, and basicity reduction of the amino group of the nucleophilic amine component (Homandberg et al., 1978).

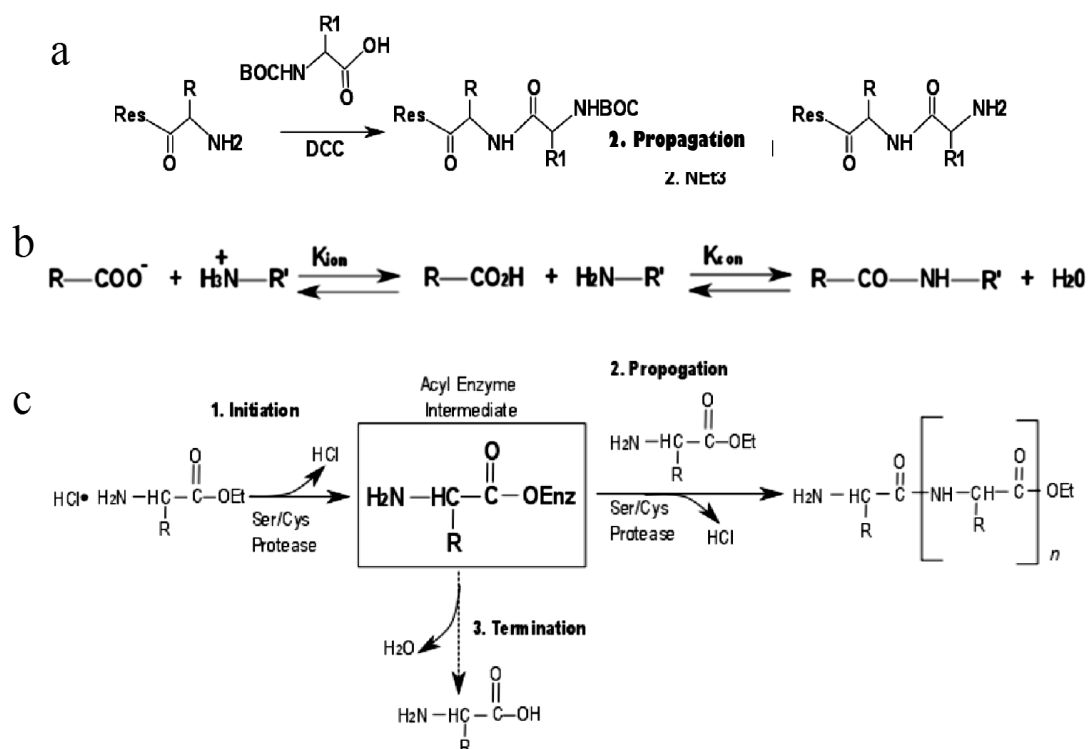


Figure 2.5 The peptide synthesis chemistry had started to gain attention followed by the chemical approach via (a) the solid-phase peptide synthesis (SPPS). Owing to the aminolysis feature of proteases, protease-mediated polypeptide synthesis has become more valuable tool in peptide synthesis chemistry through (b) a thermodynamically controlled synthesis (TCS) or (c) a kinetically controlled synthesis (KCS). Figures adapted from Baker and Numata (2013).

Types of proteases used is not restricted in the case of TCS and the protease in TCS plays important role to increase the equilibrium rate but does not change the final equilibrium (Lombard et al., 2005). TCS is a two-step process, which the first step involves an exergonic process where a proton is transferred to $-COOH$ and $-NH_2$ and followed by an endergonic condensation in second step (Figure 2.5b). Various strategies are always required to manipulate the reaction conditions in order to increase the product yield of this endergonic process. Strategies such as, product precipitation and introduction of organic solvents or water immiscible solvents, are often employed (Oyama et al., 1981). The main drawbacks of this approach are the necessity of high amount of enzyme and low reaction velocity. In contrast to TCS,

KCS requires less enzyme, short reaction time, and the product yield strongly depends on the properties and substrate specificity of the protease used. The protease used in KCS acts as a transferase, which catalyzes the transfer of an acyl group to an amino acid of peptide-derived nucleophile. In addition, KCS approach is limited to proteases that initiate the reaction through the formation of an acyl-enzyme intermediate, *e.g.* serine and cysteine proteases. Figure 2.5c describes the kinetics of KCS which is initiated by the formation of acyl-enzyme intermediate between the proteases and the ester group on modified carboxylic acid. The resulting acyl-enzyme intermediate can undergo aminolysis (propagation) as well as hydrolysis (termination) and the tendency towards either side is determined by reaction parameters such as protease activity, pH, buffer capacity, substrate concentration, and reaction time (Soeda et al., 2003; Qin et al., 2011). Numerous examples of protease-mediated synthesis of low molecular weight polypeptides have been reported so far (Li et al., 2006; Baker & Numata, 2012), however, the bulk production of high molecular weight homo- or heteropolypeptides has yet to be fulfilled.

2.2 Artificial Catalyst

As mentioned previously, enzymes are sophisticated proteins and outstanding biological catalysts with ability to accelerate the rate of chemical reactions for specific substrates and reactions. Not only catalytic efficiency, enzymes are naturally born as environmental friendly catalysts which have been a great interest especially to chemists, to involve them as an alternative to toxic chemical reagents into the field of green chemistry (Bjerre et al., 2008). Nevertheless, the use of enzymes in chemical and industrial processes is severely limited by the narrow substrate

specificity and inconveniently fast denaturation to by-products such as carbohydrates and lipids, due to the drastic changes in pH, heat or solvent, surfactants and many other chemicals during industrial processes. Obviously, if enzymes could be mimicked by chemists and applied into various extreme-conditioned industrial processes, this situation would change.

Interestingly, artificial catalyst was first fabricated to simulate and understand the relationships between the enzyme structures and functions in order to aid the exploration of the uniqueness of enzymes in contributing to the high catalytic efficiency (Breslow, 1982; Kirby, 1996). Considering a pragmatic approach to artificial catalyst, the research area of artificial catalyst was slowly expanded to the preparation of inexpensive and stable catalyst with high efficiency, as a means to overcome the limitation of natural enzymes such as, instability to heat, incompatibility with organic solvents, and so on (Murakami et al., 1996; Suh, 2003). Over the last several decades, different types of artificial catalyst including cyclodextrin (Cramer & Kampe, 1965; Lehn & Sirlin, 1978), metal complexes (Karlin et al., 1985), macromolecular scaffolds (such as crown ether (D'Souza & Bender, 1987) and porphyrins (Anderson & Sanders, 1995)), polymers (Overberger & Vorchheimer, 1963) and biomolecules (such as peptides (Atassi & Manshouri, 1993; Stavrakoudis et al., 1997) and antibodies (Lerner et al., 1991), have been explored and constructed to mimic the catalytic capabilities and fine structures of natural enzymes through various approaches (Figure 2.6).

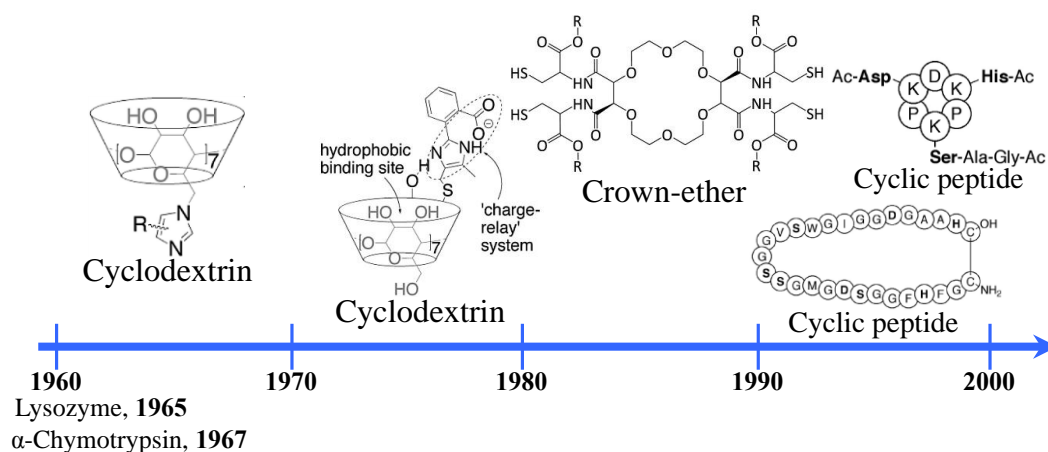


Figure 2.6 A brief timeline for the development of artificial catalysts up to year 2000. The first attempt of mimic was done on cyclodextrin with the incorporation of imidazole rings. More sophisticated designs of cyclodextrin were then introduced when 3D structures of hydrolytic enzymes such as lysozyme and α -chymotrypsin were discovered. Other artificial catalysts also including macromolecular scaffold like crown ether, as well as peptide-based mimic like cyclic peptide.

There are several features that need to be focused to facilitate efficient catalysis during the process of design and constructing artificial catalyst, which including (a) high binding affinities between enzyme and substrate, (b) high catalytic turnovers of enzyme-catalyzed reactions, and (c) substantial rate accelerations relative to uncatalyzed reactions.

High enzyme-substrate binding affinity is always the most important criteria to be considered into the construction of artificial catalyst. This is because the high catalytic efficiency of enzyme results from an optimized active site of the enzyme, which shows complementary in shape as well as charge distribution to the target substrate. The active site of enzyme contains catalytically active amino acid residues that facilitate in reaction catalysis. For example, as mentioned in the previous section, the catalytic triad of enzyme proteases, serine, aspartate, and histidine are typically found to assist intimately in catalysis (Carter & Wells, 1988). The idea of binding affinities here is not limited only to charge distributions among catalytic

residues and substrates, but also including hydrophobic binding of the substrate in the enzymatic pocket. Hydrophobic binding indicates an interaction of two hydrophobic species in a polar aqueous environment (Breslow, 2006). Due to their mutual phobia of water, the hydrophobic molecules are often attracted to each other via van der Waals attraction and hydrogen bonding (Breslow et al., 1983). Interestingly, the active sites of enzymes are usually hydrophobic, which favors hydrophobic substrates to be attracted into the interiors (Breslow, 2006) and the enzymatic reactions generally occur faster than in a hydrophilic environment. The rate acceleration in the hydrophobic environment denotes that many enzymatic mechanisms are catalyzed by general acids and bases. Generally, the reagents involved in the enzymatic reaction are solvated by water molecules in an aqueous medium and subsequently need to be desolvated in order to react with the substrate. However, the reactions that take place in the hydrophobic enzymatic pocket require less desolvation to proceed and hence increase the efficiency of catalytic action.

High catalytic turnover is another crucial feature of enzymatic catalysis and it occurs often in enzymes because they have the highest affinity towards the reaction transition state, rather than the reactants or products (Alberts et al., 2008). The formation of enzyme-substrate intermediate stabilizes the transition state and lowers the activation energy for the overall enzymatic reaction. Moreover, it has been suggested that strong binding between enzyme and the transition state is the evidence for the occurrence of covalent bond, which involves the formation of an intermediate covalently bound to the enzyme or the proton transfer occurring in the transition state. Furthermore, high concentrations of the products formed do not lead to enzymatic inhibition hence creates high catalytic turnover. Lastly, the substantial rate acceleration, which is achieved easily by enzymes, is undeniable. For example, the

decarboxylation of orotic acid undergoes 10^{17} times faster in the presence of enzyme orotidine 5'-phosphate decarboxylase as compared with its reaction in neutral aqueous solution (Radzicka & Wolfenden, 1995). This phenomenon can be highly attributed to both high substrate binding affinities and high catalytic turnovers.

Although the artificial catalysts fabricated previously have demonstrated few cases of significant efficiency and selectivity, some disadvantages still remain in such designs, for example, complicated synthetic routes, low productivity, and poor cooperativity between the catalytic centers and substrates (Yin et al., 2012). Among the aforementioned disadvantages, the structure cooperativity of natural enzymes plays a prominent role in determining the catalytic efficiency of the designed artificial catalyst (Huang et al., 2011). Against this point, Atassi and Manshouri had once designed and synthesized a cyclic peptide-based artificial catalyst of 29 amino acid residues, and proven to be almost precisely mimics the catalytic capabilities of trypsin and α -chymotrypsin (Atassi & Manshouri, 1993). Unfortunately, the attempts to reproduce the catalytic activities of cyclic peptide were failed and suggested that the poor conformational stability, which leads to the poor cooperativity between the catalytic centers and substrates, is the main drawback of this design. This finding emphasizes the pivotal importance of conformational stability between the catalytic centers and binding sites in providing a remarkable insight for the design and redesign of artificial catalysts. Impressively, introduction of new artificial catalyst design based on macromolecular scaffolds has opened up new possibilities for a better artificial catalyst construction since they can overcome the aforementioned weaknesses of the previous designs (Wolfenden & Snider, 2001; Wulff, 2002). Generally, the macromolecular-based artificial catalysts have granted the advantages: First, to carry more than one binding site as well as enough information for substrate

recognition that necessary for an efficient catalytic action. In addition, they have given high chances to meet the complementary structure between active sites and substrates via the motion of polymer chains. Eventually, macromolecular-based artificial catalysts are usually highly stable against extreme factors in terms of temperature, chemicals, and organic solvents. Followed by the discussion regarding the insights into the concept of using macromolecular-based artificial catalyst as an advantageous and effective design, some artificial catalyst construction techniques are introduced in the following sections.

2.2.1 Artificial Catalysts Based On Random Copolymers

Notably, enzymes are biological polymers created by nature concomitant with highly efficient catalytic groups. Considering the macromolecular nature of enzymes, polymers as the synthetic macromolecules possess significant advantages to become the main component for the construction of artificial catalyst. Synthetic polymer catalysts have been widely studied since the 1960s due to the physical, chemical, and biological inertness of the polymer. These properties allow the polymer to mitigate the problems that typical enzymes have in tolerating unstable reaction environments which involve subtle changes in pH and/or temperature (Suh, 2003). Polymer functionalization is a well-developed technique in which the polymer catalyst is synthesized by anchoring the corresponding functional groups onto the synthetic polymer (Kunitake & Okahata, 1976a). Amino acids, such as histidyl (imidazole) (Overberger & Vorchheimer, 1963; Saito, 1965) and cysteinyl (Komai & Noguchi, 1971) residues, that mimic the catalytic triad of an enzyme's active site are common targets for this technique. For example, imidazole-containing vinyl polymers were investigated by Kunitake *et al.* and Overberger *et al.* in the 1960s.

They found that the incorporation of imidazole derivatives—for example, 1-vinylimidazole, (Overberger & Salamone, 1969) 1-vinyl-2-methylimidazole, (Kunitake et al., 1969) 4-vinylimidazole, (Kunitake & Okahata, 1976b) and 4(5)-vinylimidazole (Overberger & Vorchheimer, 1963)—into the polymeric systems effectively enhanced the esterolytic activity.

2.2.1(a) *N*-isopropylacrylamide (NIPAm)

N-isopropylacrylamide (NIPAm) has been extensively used as the major component of polymer catalysts owing to the stimuli-responsive ability of this “smart” material, for instance, its ability to respond to different environments, such as temperature, buffer, and pH. NIPAm-based polymer catalysts in the form of a microgel, herein called NIPAm microgel (NMG), were first reported by Pelton *et al.* and were synthesized using NIPAm, acrylamide, and *N,N'*-methylenebisacrylamide without surfactant (Pelton & Chibante, 1986). The NMG was then modified by the addition of surfactants, such as sodium dodecyl sulfate (SDS) (McPhee et al., 1993; Debord & Lyon, 2003) and sodium dodecylbenzene sulfonate (NaDBS) (Ito et al., 1999), to stabilize the NMG microspheres concomitant with a smaller NMG size. This stimuli-responsive, monodispersed NMG also exhibits a volume phase transition, from a shrunken state to a swollen state and *vice versa*, at temperatures below and above the lower critical solvent temperature (LCST, typically around 30–40°C), respectively (Figure 2.7).

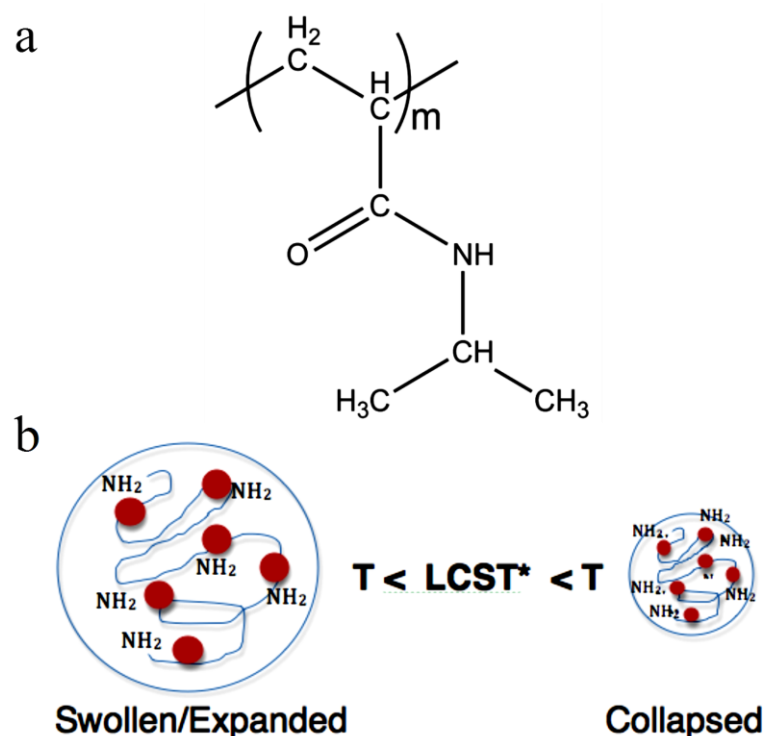


Figure 2.7 (a) Chemical structure and (b) volume phase transition of NIPAm-based microgel at temperature below and above the lower critical solvent temperature, LCST (*LCST is typically around 30–40°C).

The stimuli-responsive ability of NMG enables acceleration or deceleration of the catalytic rate, corresponding to the reaction environment in which it is situated. For example, the NIPAm-based polymer gel bearing a 4(5)-vinylimidazole functional group was synthesized by Tanaka *et al.* (Wang et al., 2000). The authors showed that gel catalysts could be switched on and off by controlling the swelling/shrinking transition of NIPAm gel in response to different solvents. The shrunken NIPAm gel successfully increased the catalytic rate with values of 0.23 mM and 0.49 h⁻¹ for Michaelis constant (K_m) and turnover rate (k_{cat}), respectively, when *p*-nitrophenyl esters were used as substrates. Furthermore, poly(NIPAm-*co*-1-vinylimidazole) synthesized by Okhapkin *et al.* (Okhapkin et al., 2004) showed a promising catalytic rate on *p*-nitrophenyl acetate (PNPA). These observations suggest that an enzyme's

catalytic triad is important in the fabrication of artificial enzymes with encouraging catalytic activity.

The functionalized NIPAm has been explored and applied to stimuli-responsive materials, such as large, reversible, pK_a shifted, and proton-imprinted NIPAm nanoparticles (NPs), with the potential to act as an active proton transporter (Hoshino et al., 2014). Furthermore, the ability of NPs to “catch and release” target proteins and peptides in response to external stimuli is of interest in developing biomedical science and biotechnology areas (Yoshimatsu et al., 2012) (Figure 2.8). However, data on the strategies used to functionalize NIPAm polymeric material through an enzyme mimic approach are limited, and further work exploring its use in robust chemical synthesis as well as in therapeutic utilities is needed. This lack of available data is partly due to difficulties in mimicking the binding mode and catalytic system of enzymes in terms of their stereochemistry, identity of functional groups, catalytic distances of various functional groups, and the mechanism of action at the enzyme active site (D’Souza & Bender, 1987). Therefore, NMG with functional groups (e.g., imidazole derivatives) need to be studied here in order to explore their potential in generating higher catalytic activity.